



Utility of high-frequency B-mode and contrast-enhanced ultrasound for the differential diagnosis of benign and malignant pleural diseases: a prospective study

Hongwei Yang^{1,2#}, Yuxin Zhang^{2#}, Dongjun Wei^{2#}, Wuxi Chen², Shiyu Zhang², Liantu He², Haixing Liao^{2*}, Qing Tang^{2*}, Jianhua Liu^{3*}

¹Department of Ultrasound, First Affiliated Hospital of Jinan University, Guangzhou, China; ²Department of Ultrasound, First Affiliated Hospital of Guangzhou Medical University, Guangzhou, China; ³Department of Medical Ultrasound, Guangzhou First People's Hospital, School of Medicine, South China University of Technology, Guangzhou, China

Contributions: (I) Conception and design: All authors; (II) Administrative support: H Liao, Q Tang, J Liu; (III) Provision of study materials or patients: Y Zhang, W Chen, D Wei; (IV) Collection and assembly of data: W Chen, D Wei, H Yang, S Zhang; (V) Data analysis and interpretation: Y Zhang, H Yang, D Wei, L He; (VI) Manuscript writing: All authors; (VII) Final approval of manuscript: All authors.

[#]These authors contributed equally to this work and should be considered as co-first authors.

^{*}These authors contributed equally to this work.

Correspondence to: Haixing Liao, MD. Department of Ultrasound, First Affiliated Hospital of Guangzhou Medical University, 151 Yanjiang Rd., Guangzhou 510120, China. Email: bluedad@163.com. Qing Tang, MD. Department of Ultrasound, First Affiliated Hospital of Guangzhou Medical University, 151 Yanjiang Rd., Guangzhou 510120, China. Email: tqgyyy@126.com. Jianhua Liu. Department of Medical Ultrasound, Guangzhou First People's Hospital, School of Medicine, South China University of Technology, Guangzhou, China. Email: liujianhua266@163.com.

Background: Pleural disease is a prevalent condition. As precision therapy advances, noninvasive imaging modalities play even more important roles in the evaluation of pleural diseases. This study investigated the diagnostic capabilities of high-frequency B-mode ultrasound (US) and contrast-enhanced US (CEUS) in terms of differentiating between benign and malignant pleural diseases.

Methods: Patients with unexplained thickened pleurae were prospectively analyzed via transthoracic US. High-frequency B-mode US was used to derive the pleural thickness, morphology, and echogenicity. We analyzed the high-frequency CEUS data including the enhancement mode and time intensity curve (TIC). The cause of pleural thickening was confirmed by pleural biopsy and follow-up after the biopsy. We analyzed the differences in various ultrasonic features between the malignant and benign groups. Moreover, we plotted receiver operator curves (ROCs) and obtained the area under the curves, sensitivities, and specificities of all significant continuous variables. Multivariate logistic regression was used to assess the combined usefulness of multiple US indicators in terms of predicting malignant pleurae.

Results: Thirty malignant and twenty benign thickened pleurae were finally diagnosed via pleural biopsy and at least six months of follow-up. The pleural morphology and enhancement modes significantly differed between the two groups (all $P < 0.05$). The thickness derived from B-mode US and CEUS were significantly thicker in the malignant group (both $P < 0.05$). Arrival time (AT) and the time to peak (TTP) of TIC were significantly shorter in the malignant group, whereas peak intensity and the area under the TIC were significantly higher in the malignant group (all $P < 0.05$). The area under the ROC for pleural thickness derived from B-mode US was 0.819; pleural thickness derived from CEUS was 0.848; AT was 0.804; TTP was 0.750; peak intensity was 0.745; the area under the TIC was 0.743; and the combined various B-mode and CEUS parameter was 0.975.

Conclusions: Pleural thickness, morphology, enhancement mode, and the TIC of high-frequency US aided the differentiation of benign from malignant pleural diseases. Combined analysis of US indicators further improved the diagnostic capability.

Keywords: Pleural disease; high-frequency ultrasound (high-frequency US); diagnostic capability

Submitted May 08, 2022. Accepted for publication Sep 23, 2022.

doi: 10.21037/jtd-22-636

View this article at: <https://dx.doi.org/10.21037/jtd-22-636>

Introduction

Pleural disease is a prevalent condition that continues to increase the global burden, thus leading to significant healthcare costs in recent years (1). Malignant pleural diseases, primarily metastases and mesothelioma, usually have poor prognoses, even with surgery (2). However, systemic comprehensive treatments including genetically targeted therapies and immunotherapy have improved the survival and quality of life of these patients (3,4). As precision therapy advances, noninvasive imaging methods play increasingly important roles in the early diagnosis and evaluation of pleural disease.

Computed tomography (CT) is the most widely used imaging modality for evaluating pleural disease. Conventional CT can be used to distinguish benign from malignant diseases based on the pleural thickness, lesion location, and calcification status (5,6). Magnetic resonance imaging (MRI) can be used to better visualize the involvement of the diaphragm and chest wall (5,6). Combining dynamic contrast-enhanced CT and contrast-enhanced MRI further improves the diagnostic efficiency and is useful for evaluating the patient response to drug therapy for pleural lesions (7,8). Positron emission tomography computed tomography (PET/CT) plays an important role in the diagnosis and staging of malignant pleural mesothelioma (9). However, all these imaging modalities are time-consuming and are not readily acceptable for repeat examinations or follow up. For example, the radiation risks posed by CT and PET/CT, the motion artifacts in MRI, as well as imaging-specific medical expenses with these modalities, hinders their widespread use in the clinical setting.

Ultrasound (US) is a cost-effective and nonradiative approach that can be used for point-of-care evaluation. Until two decades ago, ultrasonography was perceived to be of low-efficiency in diagnosing chest diseases because of the alveolar gas-liquid interference in the lung. However, the pleura of the outer layer of the lung is clear in US performed through the soft tissue acoustic window of the chest wall; pleural effusion affords excellent contrast. Today, the relevant guidelines recommended US as the preferred imaging modality for pleural effusion and first-line imaging to guide thoracentesis and pleural biopsy (10-12). B-mode

pleural thickness and morphology, as revealed by low-frequency probes, can distinguish between benign and malignantly thickened pleurae (13). However, the pleura is a relatively superficial organ, and the value of high-frequency US in the diagnosis of pleural diseases is uncertain.

Given the widespread availability of contrast-enhanced US (CEUS), its utility in terms of diagnosing pleural diseases deserves more attention. Second-generation US microbubble contrast agents yield image series within which the contrast varies. The devices employ a low mechanical index technique to detect tissue perfusion with high temporal and spatial resolution. CEUS lacks the respiratory motion artifacts of Doppler US (14). Moreover, it facilitates parameter quantification using a time-enhancement curve, and it is good at distinguishing between benign and malignant diseases of the lung and liver (15,16). However, its diagnostic utility in terms of differentiating between benign and malignant thickened pleurae remains unclear.

Therefore, in this study, we evaluated the diagnostic capabilities of high-frequency US (including B-mode US and CEUS) in terms of differentiating between benign and malignant pleural diseases. We present the following article in accordance with the STARD reporting checklist (available at <https://jtd.amegroups.com/article/view/10.21037/jtd-22-636/rc>).

Methods

Study design

The study was conducted in accordance with the Declaration of Helsinki (as revised in 2013). This prospective single-center study was approved by the Scientific Research Ethics Review Committee of the First Affiliated Hospital of Guangzhou Medical University (No. 2020-21). Informed consent was obtained from each patient. The inclusion criteria were pleural thickening (≥ 3 mm) or a pleural lesion, a diagnosis of pleural pathology, no prior anti-tumor treatment, patient consent, and age >18 years. The exclusion criteria were any history of hypersensitivity to a CEUS agent, an inability to undergo CEUS because of tachypnea, a lesion located in the lung or chest wall, unclear US images, or insufficient data.

All patients included in this study were treated at our

medical center for unexplained pleural effusion or pleural thickening. US evaluation of pleurae was performed before all invasive diagnostic methods (thoracentesis, percutaneous biopsy, or thoracoscopy). Consecutive patients were analyzed via transthoracic US (Resona 7T; Mindray, Shenzhen, China) with SC5-1U probe (1.2–6.0 MHz) and L9-3U probe (2.5–9.0 MHz) during the period from January 2020 to August 2021. The low-frequency probe (SC5-1U) was initially used to scan all rib spaces individually. When a thickened pleura was found, B-mode US using a high-frequency probe (L9-3U) was used to derive the pleural thickness, morphology, and echogenicity. Then, the thickest pleural area/lesion was subjected to CEUS using a high-frequency probe. A 2.4 mL bolus of contrast agent (Sonovue; Bracco, Milan, Italy) was intravenously injected followed by a 5.0 mL saline flush; then, the pleural area was continuously observed for 180 s. All data were stored.

Data analysis and collection

B-mode US and CEUS parameters were evaluated by two sonographers (working in consensus; each with at least 5 years of experience with CEUS and thoracic US examination) who were blinded to the pleural pathological diagnosis. The maximum pleural thickness was measured via both B-mode US and CEUS using high-frequency probes. Compared to the chest wall, pleural echogenicity as viewed via B-mode US was classified as hyperechoic, isoechoic, or hypoechoic. Pleural thickening was categorized as uniform, wavy/papillary, or mass-like.

The CEUS data analyzed included the enhancement mode and the time intensity curve (TIC). The possible enhancement modes were homogeneous, centripetal (peripheral enhancement that increased gradually toward the center), and inhomogeneous. We used the software of TIC quantitative analysis in the US machine (Resona 7T). When patients underwent US-guided pleural needle biopsy, the regions of interest of the TICs were placed in the needle puncture paths, and the arrival time (AT), time to peak (TTP), peak intensity (PI), and the area under the TIC were automatically determined.

Final diagnoses

A malignancy was confirmed via surgical resection or pleural biopsy. A diagnosis of benign was made via surgical

resection (at least two benign results of percutaneous pleural biopsies within 1 month, or a benign biopsy followed-up by at least 6 months of imaging). According to the final diagnosis, we divided the cases into a malignant group and benign group.

Statistical analysis

SPSS version 22.0 software was used for all analyses. Quantitative data are presented as mean \pm standards deviation and were compared using an independent samples *t*-test and rank sum test (the Wilcoxon test). We calculated Spearman's correlation coefficient between pleural thickness consistencies measured via B-mode US and CEUS. Moreover, we analyzed the differences in various ultrasonic features between the malignant group and benign group. Further, we plotted the receiver operator curves (ROCs) and obtained the area under curves (AUCs,) cutoffs, sensitivities, and specificities of all significant continuous variables. Multivariate logistic regression was used to assess the combined utilities of multiple US indicators in terms of predicting malignant pleurae. A *P* value <0.05 was considered to indicate a significant difference.

Results

Patient characteristics

Sixty-one patients with thickened pleurae were initially evaluated but eleven were excluded (*Figure 1*) because the masses were in the chest wall or lung ($n=2$), the images were of poor quality because of thick chest walls ($n=2$), consecutive CEUS scans were less than 3 minutes ($n=2$), and stable TICs were not obtained because of severe coughing or tachypnea ($n=5$). Final diagnoses contained 20 cases of benign pleural disease and 30 of malignant pleural disease during the period from January 2020 to August 2021 (*Table 1*). All malignant cases were diagnosed by results of percutaneous pleural biopsy. All benign cases were confirmed by one benign result of percutaneous pleural biopsy and at least six months of follow-up. The patients with malignant disease included 20 men and 10 women with a mean age of 58.1 ± 14.4 years, of whom 23 evidenced pleural effusion and 7 did not. The patients with benign disease included 17 men and 3 women with a mean age of 58.4 ± 17.0 years, of whom 17 evidenced pleural effusion and 3 did not. Age, sex, and pleural effusion status did not differ between the two groups (*Table 2*).

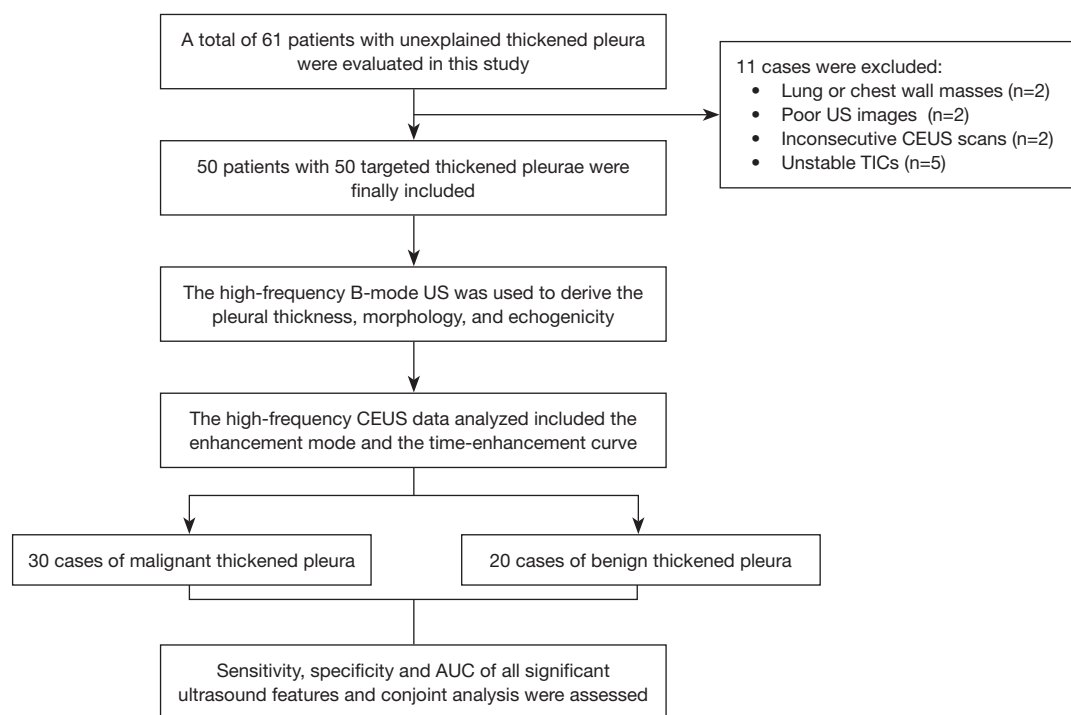


Figure 1 Flow diagram of the cases selection and analysis process. CEUS, contrast-enhanced ultrasound; TIC, time intensity curve; US, ultrasound; AUC, area under the curve.

Table 1 The final diagnosis of all patients

Types of diagnosis	Number of case
Malignant thickened pleura	30
Malignant mesothelioma	3
Metastatic carcinoma	22
Metastatic lung adenocarcinoma	18
Metastatic lung squamous cell carcinoma	3
Metastatic small cell lung cancer	1
Other malignant pleural diseases	5
Benign thickened pleura	20
Tuberculosis or granulomatous inflammation	7
Nonspecific inflammation	13
Total	50

B-mode US data

Of the 30 malignant pleurae, the average thickness was 13.4 ± 11.0 mm according to B-mode US; 13 exhibited uniform, 7 exhibited wavy/papillary, and 10 exhibited

mass thickening (the latter included all the mesothelioma cases). Of all malignant pleurae, 19 were hypoechoic, 7 were isoechoic, and 4 were hyperechoic. Of the 20 benign pleurae, the average pleural thickness was 5.2 ± 1.5 mm according to B-mode US; only one evidenced wavy/papillary thickening, all others exhibited homogeneous thickening. There were 16 hypoechoic and 4 isoechoic pleurae. The echo type did not differ significantly between the benign and malignant groups, but the pleural morphology and thickness derived from B-mode US did (both $P < 0.05$). The details are shown in *Table 2*.

CEUS data

Of the 30 malignant pleurae, the average thickness was 13.4 ± 10.5 mm according to CEUS examination; 9 (30%) exhibited homogeneous, 11 (36.7%) exhibited centripetal, and 10 (33.3%) exhibited inhomogeneous enhancement. Of the 20 benign cases, the average pleural thickness was 5.3 ± 1.7 mm according to CEUS examination; 14 (70%) exhibited homogeneous, 1 (5%) exhibited centripetal, and 5 (25%) exhibited inhomogeneous enhancement. The enhancement mode and pleural thickness derived from

Table 2 Demographics and ultrasound characteristics between malignant and benign pleural groups

Characteristics	Benign group (n=20)	Malignant group (n=30)	P value
Age (year) [†]	58.4±17.0	58.1±14.4	0.950
Sex			0.131
Male	17	20	
Female	3	10	
Pleural effusion			0.365
Yes	7	23	
No	3	7	
Thickness in B-mode US (mm) [†]	5.2±1.5	13.4±11.0	<0.001*
Thickness in CEUS (mm) [†]	5.3±1.7	13.4±10.5	<0.001*
Pleural morphology			0.001*
Uniform	19	13	
Wavy/papillary	1	7	
Mass	0	10	
Echogenicity			0.202
Hypoechoic	16	19	
Isoechoic	4	7	
Hyperechoic	0	4	
Enhancement mode			0.011*
Homogeneous	14	9	
Centripetal	1	10	
Inhomogeneous	5	11	

[†], data are means ± standard deviations; *, statistically significant (P<0.05). US, ultrasound; CEUS, contrast-enhanced ultrasound.

Table 3 Quantitative analysis of time intensity curve from pleural CEUS

Parameters	Benign group	Malignant group	P value
AT(s)	19.3±5.7	13.2±4.0	<0.001*
TTP(s)	38.3±10.0	30.0±7.4	0.001*
PI	19.5±6.4	26.3±7.7	0.002*
Area under the TIC	2,337.1±765.9	3,328.6±1,317.7	0.002*

*, statistically significant (P<0.05). AT, TTP, PI and area under the TIC were expressed as mean ± standard deviation. CEUS, contrast-enhanced ultrasound; AT, arise time; TTP, time to peak; PI, peak intensity; TIC, time intensity curve.

CEUS differed significantly between the two groups (both P<0.05). The details are shown in *Table 2*.

In terms of the TIC parameters of the malignant group, the average AT was 13.2±4.0 s, the average TTP was 30.0±7.4 s, the average PI was 26.3±7.7, and the average area under the TIC was 3,328.6±1,317.7; in the benign

group, the values were 19.3±5.7, 38.3±10.0, 19.5±6.4, and 2,337.1±765.9 s, respectively. Together the AT and TTP were significantly shorter in the malignant group than in the benign group, whereas the PI and the area under the TIC were significantly higher in the malignant group (all P<0.05). The details are shown in *Table 3*.

Diagnostic capabilities of individual and combined US features

The cutoff value for pleural thickness derived from high-frequency B-mode US was 7.3 mm, with a sensitivity of 63.3%, specificity of 90.0%, and an AUC of 0.819 [95% confidence interval (CI): 0.696 to 0.942]. The cutoff value for high-frequency CEUS-derived pleural thickness was 7.9 mm with a sensitivity of 70.0%, specificity of 95.0%, and an AUC of 0.848 (95% CI: 0.740 to 0.957). Both US modes exhibited good consistency when used to measure pleural thicknesses (related coefficient: 0.965, $P < 0.001$).

The AT cutoff was 16.8 s with a sensitivity of 83.3%, specificity of 65.0%, and an AUC of 0.804 (95% CI: 0.674 to 0.935). The TTP cutoff was 37.3 s with a sensitivity of 86.7%, specificity of 70.0%, and an AUC of 0.750 (95% CI: 0.608 to 0.892). The PI cutoff was 25.8 with a sensitivity of 56.7%, specificity of 90.0%, and an AUC of 0.745 (95% CI: 0.610 to 0.880). The cutoff of area under the TIC was 3,590.1 with a sensitivity of 43.3%, specificity of 100.0%, and an AUC of 0.743 (95% CI: 0.609 to 0.877).

Multivariate logistic regression was performed in the multiparameter combined diagnosis. According to the predicted value of the joint diagnostic index obtained by multivariate logistic regression, ROC of multiparameter combined diagnosis was performed. The sensitivity, specificity, and AUC of the combined pleural thickness derived from CEUS, morphology, CEUS enhancement mode, AT, TTP, PI, and the area under the TIC, were 93.3%, 90.0%, and 0.975 (95% CI: 0.940 to 1.000), respectively. The ROCs of all parameters are shown in *Figure 2*.

Discussion

US pleural evaluation affords certain advantages; the pleura lies shallowly, no lung gas is present, and pleural effusion affords contrast. However, US has not been widely used to diagnose pleural diseases. Although only 50 cases were included in this study, this study still included most types of diseases that can lead to pleural thickening (see *Table 1*), and the sample size of our study was basically similar to previous studies about pleural US (13,17). We performed a prospective analysis and found that both high-frequency B-mode US and CEUS were able to clearly distinguish between benign and malignant thickened pleurae. Additionally, this study also report that a combination of measurements obtained via high-frequency B-mode US and CEUS improves the differentiation of benign from

malignant pleural diseases.

Pleural thickness and morphology (assessed via US, CT, or MRI) are commonly used to distinguish between benign and malignant pleurae (5,6,13). Qureshi *et al.* reported that pleural thickening >1 cm and diaphragmatic thickening >7 mm were highly suggestive of malignant pleural disease (13). However, a recent study showed that the selection of 15 mm as a cut-off value yielded a sensitivity of 78.6%, a specificity of 74.1%, and an AUC of 0.714 in diagnosing malignant pleural disease (17). We also found that malignant pleurae were significantly thicker than benign pleurae. However, different from previous studies, the value of high-frequency US is the focus of our study. For B-mode US, the benign/malignant thickness cutoff was 7.3 mm with a sensitivity of 63.3%, a specificity of 90.0%, and an AUC of 0.819. For CEUS, the cutoff was 7.9 mm with a sensitivity of 70.0%, a specificity of 95.0%, and an AUC of 0.819. Although the cut-off value of pleural thickness proposed in our study was thinner than that reported in previous studies, the cut-off value of pleural thickness in our study afforded a high specificity and AUC when distinguishing between benign and malignant pleural diseases. In addition, we also used two US modes to evaluate all patients and found that the high-frequency B-mode US data were in excellent agreement with those of CEUS. Therefore, we considered that high-frequency US reveals pleural details and could also be used to guide percutaneous biopsy. Moreover, we found that malignant pleurae exhibited wavy/papillary and mass thickening; all three mesotheliomas evidenced the latter type of thickening. Although benign pleural diseases also show evidence of thickening, this is commonly uniform, perhaps because the thickening is principally exudative fibrous or tuberculosis granulation tissue hyperplasia (which is generally uniform). However, malignant pleural thickening caused by tumors is accompanied by local erosion and destruction, thus resulting in nodules and/or mass-like changes.

It is difficult to ascertain the pleural distributions of blood vessels using Doppler US because of respiratory motion artifacts and the relatively thin tissue (14,18). However, CEUS is good at detecting microvessels and is not affected by motion artifacts. Several studies have found that CEUS is useful for diagnosing subpleural lung lesions (15,19-21). However, the blood supplies to the pleura and peripheral lung lesions differ. The efficacy of CEUS in terms of pleural disease diagnosis remains unproven. Although previous studies reported that marked enhancement was significantly more frequently

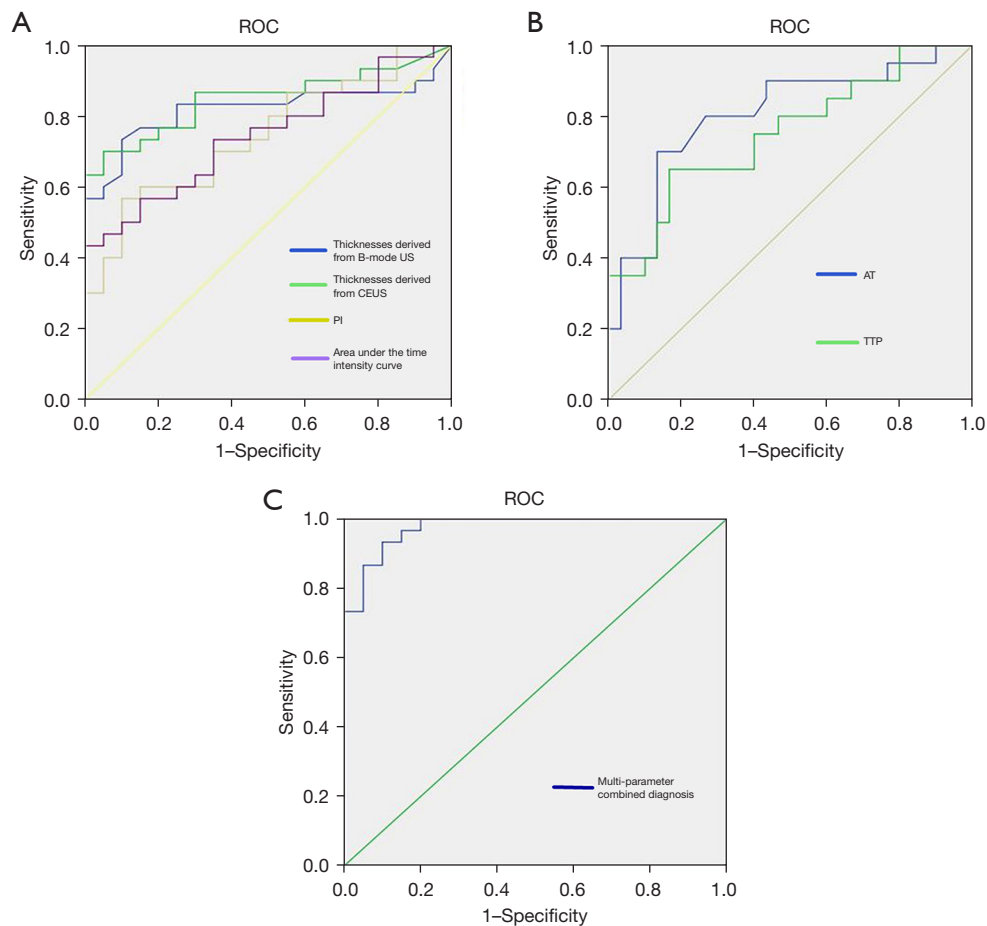


Figure 2 The ROCs of all significant continuous variables and combined diagnosis were plotted. (A) ROCs analysis of PI, area under the time intensity curve, and the thicknesses derived from B-mode US and CEUS for predicting malignant thickened pleurae. (B) ROCs analysis of AT and TTP for predicting malignant thickened pleurae. (C) ROCs analysis of multi-parameter combined diagnosis for predicting malignant thickened pleurae. ROC, receiver operator curve; US, ultrasound; CEUS, contrast-enhanced ultrasound; PI, peak intensity; AT, arrival time; TTP, time to peak.

associated with malignant compared with benign lesions, the enhancement pattern and TIC of the pleurae were not investigated in the retrospective study (17,22). In the present prospective study, we found that the enhancement mode and quantitative data from the TIC usefully aided the differential diagnosis of benign and malignant pleural diseases. We found the average AT of malignant pleural disease was 13.2 ± 4.0 s, which was significantly less than 19.3 ± 5.7 s (average AT of benign pleural disease). This indicates that the contrast agent entered into the malignant thickened pleura faster than benign thickened pleura. In addition, the TTP of malignant pleural disease was also found to be significantly less than that of benign pleural disease (30.0 ± 7.4 vs. 38.3 ± 10.0 s, $P < 0.05$). When the

enhancement intensity reaches the peak, this means that the intensity begins to weaken. Therefore, this indicates that the contrast agent washed out faster in the malignant thickened pleura than that of benign thickened pleura. Although both pleural tumors and subpleural lung tumors are located in the chest, malignant pleural disease tended to exhibit “fast-in/fast-out” enhancement (see *Figures 3,4*), unlike the “slow-in/fast-out” enhancement of peripheral lung cancer (15,19-21). In addition, we also found that the PI and the area under the TIC of malignant pleural disease were significantly higher than those of benign pleural disease. Compared with previous studies (17,22), our result further confirmed that marked enhancement was significantly more frequently associated with malignant

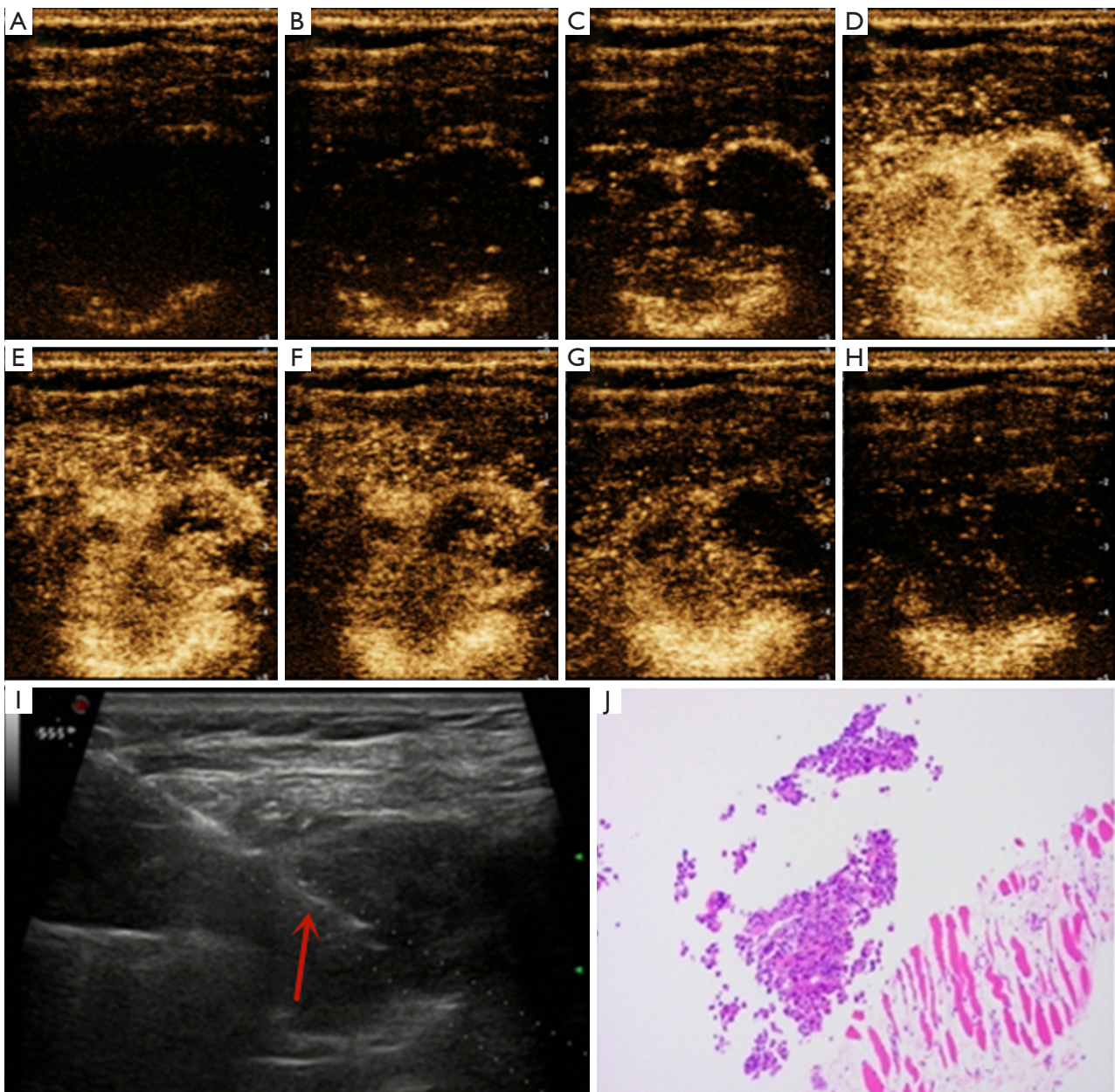


Figure 3 Images of a 47-year-old man diagnosed with pleural metastasis of lung adenocarcinoma. (A) Enhancement at 1 s. (B) Enhancement at 11 s. (C) Enhancement at 14 s. (D) Enhancement at 18 s. (E) Enhancement at 23 s. (F) Enhancement at 34 s. (G) Enhancement at 1 min 22 s. (H) Enhancement at 3 min. (A-H) Contrast enhanced ultrasound showed centripetal enhancement and “fast-in/fast-out” enhancement. (I) Ultrasound guided percutaneous needle pleural biopsy; red arrow: needle. (J) Pathological diagnosis: adenocarcinoma (H&E, $\times 100$).

compared with benign pleural disease, from the perspective of precise quantitative analysis. Furthermore, although the malignant pleural disease evidenced several enhancement modes, the benign pleural disease seldom exhibited centripetal enhancement, which may thus be rather specific for pleural disease (Figures 3,4). TIC was also innovatively

used to conduct accurate quantitative analysis of pleural enhancement in this study, so as to avoid the differences in the observation of enhancement mode between different observers. In general, we are the first to show that the TIC of CEUS is highly useful for the differential diagnosis of benign and malignant pleural diseases.

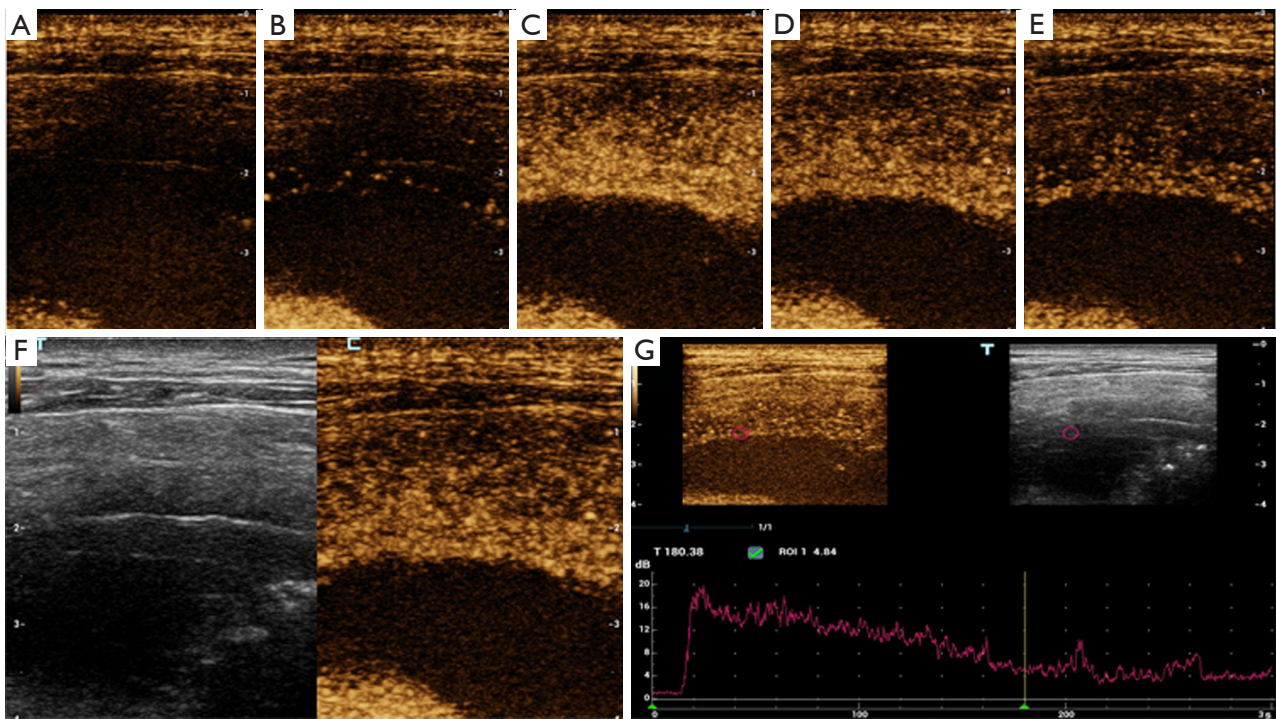


Figure 4 Images of a 71-year-old female diagnosed with benign pleural disease. (A) Enhancement at 10 s. (B) Enhancement at 15 s. (C) Enhancement at 26 s. (D) Enhancement at 1 min. (E) Enhancement at 2 min 20 s. (A-E) Contrast enhanced ultrasound showed homogeneous “slow-in/slow-out” enhancement. (F) B-mode ultrasound and contrast enhanced ultrasound showed the uniformly thickened pleura. (G) Analysis of time-enhancement curves; arise time: 13.6 s, time to peak: 39.2 s, peak intensity: 15.8, and area under the curve: 1,936.7.

Although we found several US features that aided in the differentiation of benign from malignant pleural disease, most diagnoses are multimodal. It is important to consider the different benefits that various imaging modes may offer. The thickness and shape of two-dimensional US may be the most commonly imaging features to diagnose the pleural disease. However, although the thickness and shape of pleura may not be abnormal in the early stage of malignant pleural disease, the microvessels or blood supply in the pleura may have changed. For those cases with thin pleura, CEUS may be helpful. In our cases, some patients with malignant pleural disease did not have pleural thickening (<7.3 mm), but the mode and quantitative parameters of CEUS showed malignant characteristics. On the contrary, the CEUS patterns between benign and malignant pleural diseases may have some overlap, but the thickness and shape of pleura may be helpful for the differential diagnosis of benign and malignant pleural diseases. Therefore, we further used combinations of US parameters to identify benign and malignant pleural diseases. The sensitivity, specificity, and AUC increased (to 93.3%, 90.0%, and

0.975, respectively) when we combined thickness derived from CEUS, morphology, and enhancement mode along with several quantitative parameters yielded by the TIC. The AUC improved markedly compared to single-feature values (*Figure 2*). However, combined diagnosis is rather cumbersome. Single US indicators still play useful roles. The US mode should be chosen based on the clinical situation and the diagnostic requirements.

Our work has certain limitations. First, this is a study with a small sample size. Second, pleura less than 3 mm was not included in this study. Lastly, we mostly focused on the parietal pleurae; we studied only a few visceral pleurae.

In conclusion, pleural thickness and morphology, the enhancement mode, and the TIC of high-frequency US aided in the differentiation of benign from malignant pleural diseases; combined analysis of US indicators further improved the diagnostic capability.

Acknowledgments

The language of the article was edited by the English

professional from Editage.

Funding: This work was supported by Science and Technology Program of Guangzhou, China (No. 202201020433), Science and Technology Planning Project of Guangdong Province, China (grant No. 2017A020215062) and Medical Scientific Research Foundation of Guangdong Province, China (grant No. A2020408).

Footnote

Reporting Checklist: The authors have completed the STARD reporting checklist. Available at <https://jtd.amegroups.com/article/view/10.21037/jtd-22-636/rc>

Data Sharing Statement: Available at <https://jtd.amegroups.com/article/view/10.21037/jtd-22-636/dss>

Conflicts of Interest: All authors have completed the ICMJE uniform disclosure form (available at <https://jtd.amegroups.com/article/view/10.21037/jtd-22-636/coif>). The authors have no conflicts of interest to declare.

Ethical Statement: The authors are accountable for all aspects of the work in ensuring that questions related to the accuracy or integrity of any part of the work are appropriately investigated and resolved. The study was conducted in accordance with the Declaration of Helsinki (as revised in 2013). The study was approved by the Scientific Research Ethics Review Committee of the First Affiliated Hospital of Guangzhou Medical University (No. 2020-21) and the informed consent was obtained from each patient.

Open Access Statement: This is an Open Access article distributed in accordance with the Creative Commons Attribution-NonCommercial-NoDerivs 4.0 International License (CC BY-NC-ND 4.0), which permits the non-commercial replication and distribution of the article with the strict proviso that no changes or edits are made and the original work is properly cited (including links to both the formal publication through the relevant DOI and the license). See: <https://creativecommons.org/licenses/by-nc-nd/4.0/>.

References

- Bhatnagar R, Corcoran JP, Maldonado F, et al. Advanced medical interventions in pleural disease. *Eur Respir Rev* 2016;25:199-213.
- Feller-Kopman DJ, Reddy CB, DeCamp MM, et al. Management of Malignant Pleural Effusions. An Official ATS/STS/STR Clinical Practice Guideline. *Am J Respir Crit Care Med* 2018;198:839-49.
- Chen Y, Mathy NW, Lu H. The role of VEGF in the diagnosis and treatment of malignant pleural effusion in patients with non-small cell lung cancer (Review). *Mol Med Rep* 2018;17:8019-30.
- Gounant V, Brosseau S, Zalzman G. Immunotherapy, the promise for present and future of malignant pleural mesothelioma (MPM) treatment. *Ther Adv Med Oncol* 2021;13:17588359211061956.
- Bianco A, Valente T, De Rimini ML, et al. Clinical diagnosis of malignant pleural mesothelioma. *J Thorac Dis* 2018;10:S253-61.
- Hierholzer J, Luo L, Bittner RC, et al. MRI and CT in the differential diagnosis of pleural disease. *Chest* 2000;118:604-9.
- Coolen J, De Keyzer F, Naftoux P, et al. Malignant pleural disease: diagnosis by using diffusion-weighted and dynamic contrast-enhanced MR imaging--initial experience. *Radiology* 2012;263:884-92.
- Gudmundsson E, Labby Z, Straus CM, et al. Dynamic contrast-enhanced CT for the assessment of tumour response in malignant pleural mesothelioma: a pilot study. *Eur Radiol* 2019;29:682-8.
- Kruse M, Sherry SJ, Paidpally V, et al. FDG PET/CT in the management of primary pleural tumors and pleural metastases. *AJR Am J Roentgenol* 2013;201:W215-26.
- van Zandwijk N, Clarke C, Henderson D, et al. Guidelines for the diagnosis and treatment of malignant pleural mesothelioma. *J Thorac Dis* 2013;5:E254-307.
- Davies HE, Davies RJ, Davies CW, et al. Management of pleural infection in adults: British Thoracic Society Pleural Disease Guideline 2010. *Thorax* 2010;65 Suppl 2:ii41-53.
- Scherpereel A, Opitz I, Berghmans T, et al. ERS/ESTS/EACTS/ESTRO guidelines for the management of malignant pleural mesothelioma. *Eur Respir J* 2020;55:1900953.
- Qureshi NR, Rahman NM, Gleeson FV. Thoracic ultrasound in the diagnosis of malignant pleural effusion. *Thorax* 2009;64:139-43.
- Zhou JH, Shan HB, Ou W, et al. Contrast-Enhanced Ultrasound Improves the Pathological Outcomes of US-Guided Core Needle Biopsy That Targets the Viable Area of Anterior Mediastinal Masses. *Biomed Res Int* 2018;2018:9825709.
- Bi K, Xia DM, Fan L, et al. Development and Prospective Validation of an Ultrasound Prediction Model for the

- Differential Diagnosis of Benign and Malignant Subpleural Pulmonary Lesions: A Large Ambispective Cohort Study. *Front Oncol* 2021;11:656060.
16. Strobel D, Jung EM, Ziesch M, et al. Real-life assessment of standardized contrast-enhanced ultrasound (CEUS) and CEUS algorithms (CEUS LI-RADS®/ESCU LAP) in hepatic nodules in cirrhotic patients—a prospective multicenter study. *Eur Radiol* 2021;31:7614-25.
 17. Findeisen H, Görg C, Hartbrich R, et al. Contrast-enhanced ultrasound is helpful for differentiating benign from malignant parietal pleural lesions. *J Clin Ultrasound* 2022;50:90-8.
 18. Zhang Y, Tang J, Zhou X, et al. Ultrasound-guided pleural cutting needle biopsy: accuracy and factors influencing diagnostic yield. *J Thorac Dis* 2018;10:3244-52.
 19. Tang M, Xie Q, Wang J, et al. Time Difference of Arrival on Contrast-Enhanced Ultrasound in Distinguishing Benign Inflammation From Malignant Peripheral Pulmonary Lesions. *Front Oncol* 2020;10:578884.
 20. Sperandeo M, Sperandeo G, Varriale A, et al. Contrast-enhanced ultrasound (CEUS) for the study of peripheral lung lesions: a preliminary study. *Ultrasound Med Biol* 2006;32:1467-72.
 21. Lei Z, Lou J, Bao L, et al. Contrast-enhanced ultrasound for needle biopsy of central lung cancer with atelectasis. *J Med Ultrason (2001)* 2018;45:461-7.
 22. Safai Zadeh E, Weide J, Dietrich CF, et al. Diagnostic Accuracy of B-Mode- and Contrast-Enhanced Ultrasound in Differentiating Malignant from Benign Pleural Effusions. *Diagnostics (Basel)* 2021;11:1293.

Cite this article as: Yang H, Zhang Y, Wei D, Chen W, Zhang S, He L, Liao H, Tang Q, Liu J. Utility of high-frequency B-mode and contrast-enhanced ultrasound for the differential diagnosis of benign and malignant pleural diseases: a prospective study. *J Thorac Dis* 2022;14(10):3695-3705. doi: 10.21037/jtd-22-636